

Supplementary materials for: Improving aerosol activation in the double-moment Unified Model with CLARIFY measurements

Hamish Gordon^{1,2}, Paul R. Field^{1,3}, Steven J. Abel³, Paul Barrett³, Keith Bower⁴, Ian Crawford⁴, Zhiqiang Cui¹, Daniel P. Grosvenor¹, Adrian A. Hill³, Jonathan Taylor⁴, Jonathan Wilkinson³, Huihui Wu⁴, and Ken S. Carslaw¹

- 5
1. School of Earth and Environment, University of Leeds, LS2 9JT, United Kingdom
 2. Engineering Research Accelerator, Carnegie Mellon University, Forbes Avenue, Pittsburgh 15213, United States
 3. Met Office, Fitzroy Road, Exeter, EX1 3PB, United Kingdom
 4. Department of Earth and Environmental Sciences, University of Manchester, M13 9PL, United Kingdom

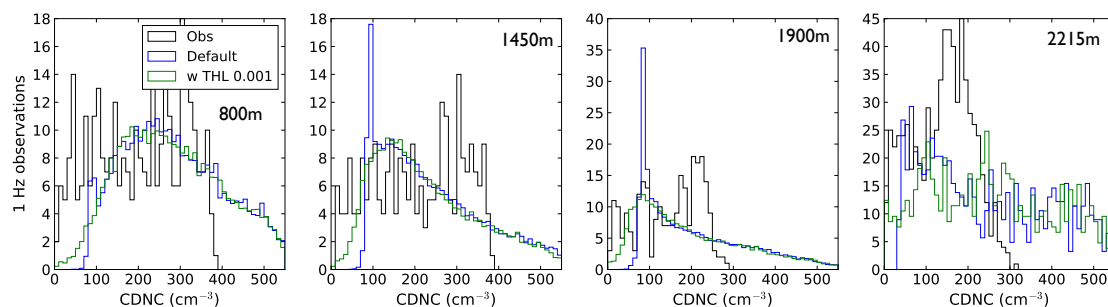


Figure S1. Change in droplet concentration when the updraft PDF threshold of 0.1m/s is reduced to 0.001m/s at 500 m resolution.

Table S1. Mean in-cloud liquid water content in observations from the cloud droplet probe, compared to the default version of the model. In both model and observations, the threshold liquid water content is 0.01 g/kg to define a cloud.

Altitude	Obs (g/kg)	Model (g/kg)
800	0.34	0.07
1450	0.42	0.13
1900	0.58	0.18
2215	0.68	0.58
2550	0.70	0.98

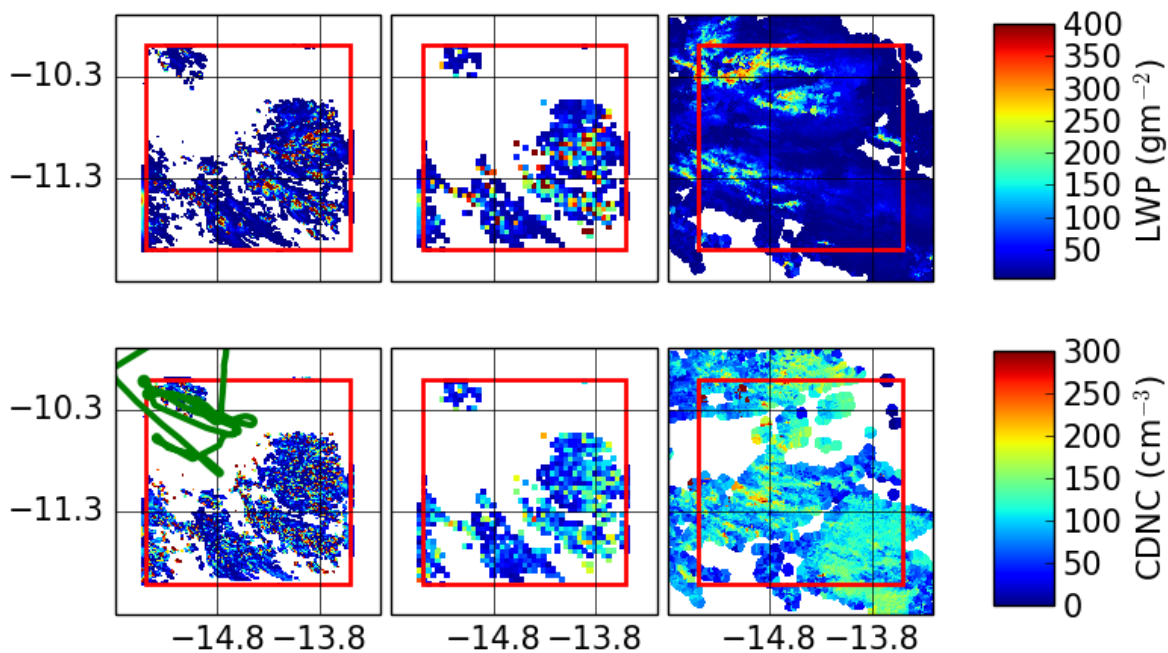


Figure S2. As Figure 3, except that the central subfigures show the 500 m simulation regridded to 5 km resolution, for a potentially fairer comparison with MODIS

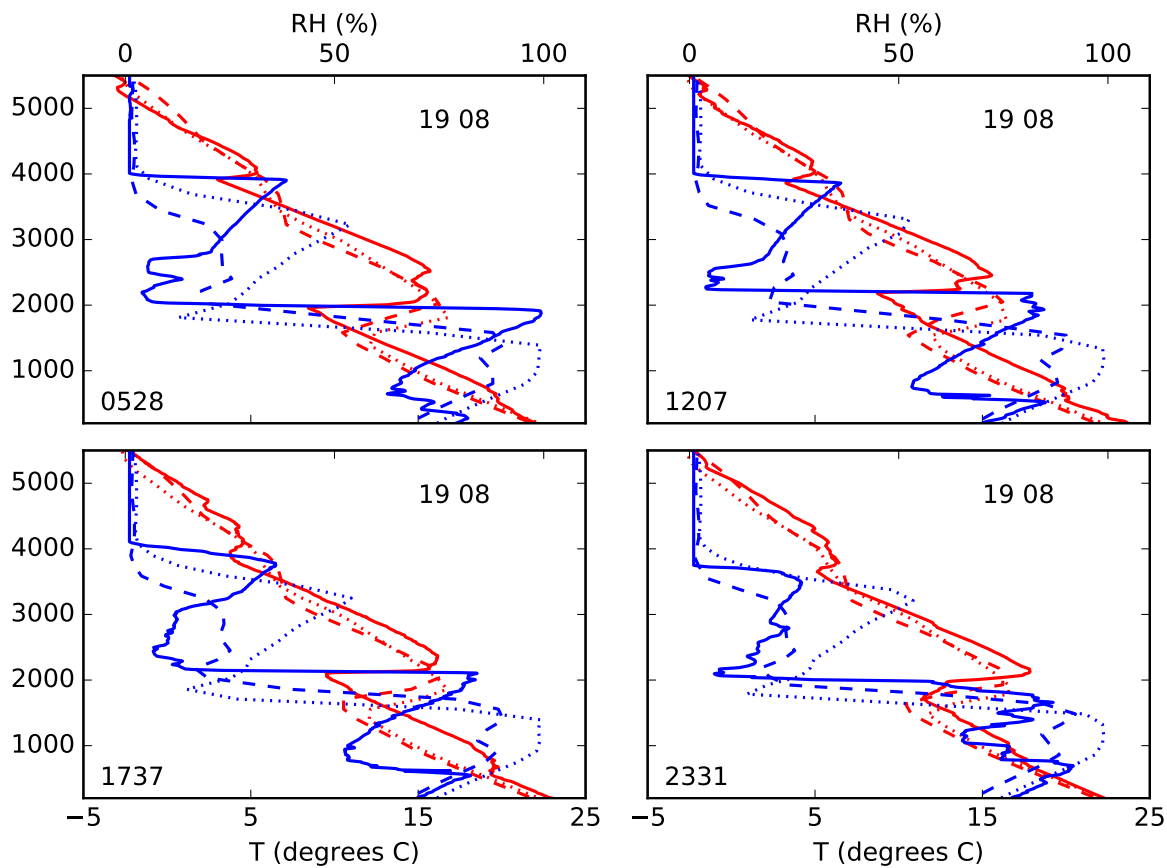


Figure S3. Driving model evaluation against Ascension Island radiosondes on 19 August. The global model is shown with the dashed line and the 7 km regional model with the dotted line. To reduce computational expense, the domain we simulate at 500 m resolution does not include Ascension Island.

Table S2. Mean and standard deviation of in-cloud updraft speed in observations and in simulations, split by LWC

Altitude (m)	\bar{w} obs. ms^{-1}	\bar{w} model ms^{-1}	σ_w obs. ms^{-1}	σ_w 500 m ms^{-1}
800	0.69	0.98	1.32	0.90
1450	0.75	0.51	1.40	0.92
1900	0.72	0.17	1.47	0.73
2215	0.04	0.07	1.63	1.00
2550	-0.61	0.17	2.80	1.37
800	-0.006	0.12	0.88	0.34
1450	-0.12	-0.012	1.10	0.25
1900	-0.88	-0.04	0.92	0.22
2215	-0.42	-0.15	1.39	0.49
2550	-0.90	0.52	2.35	-

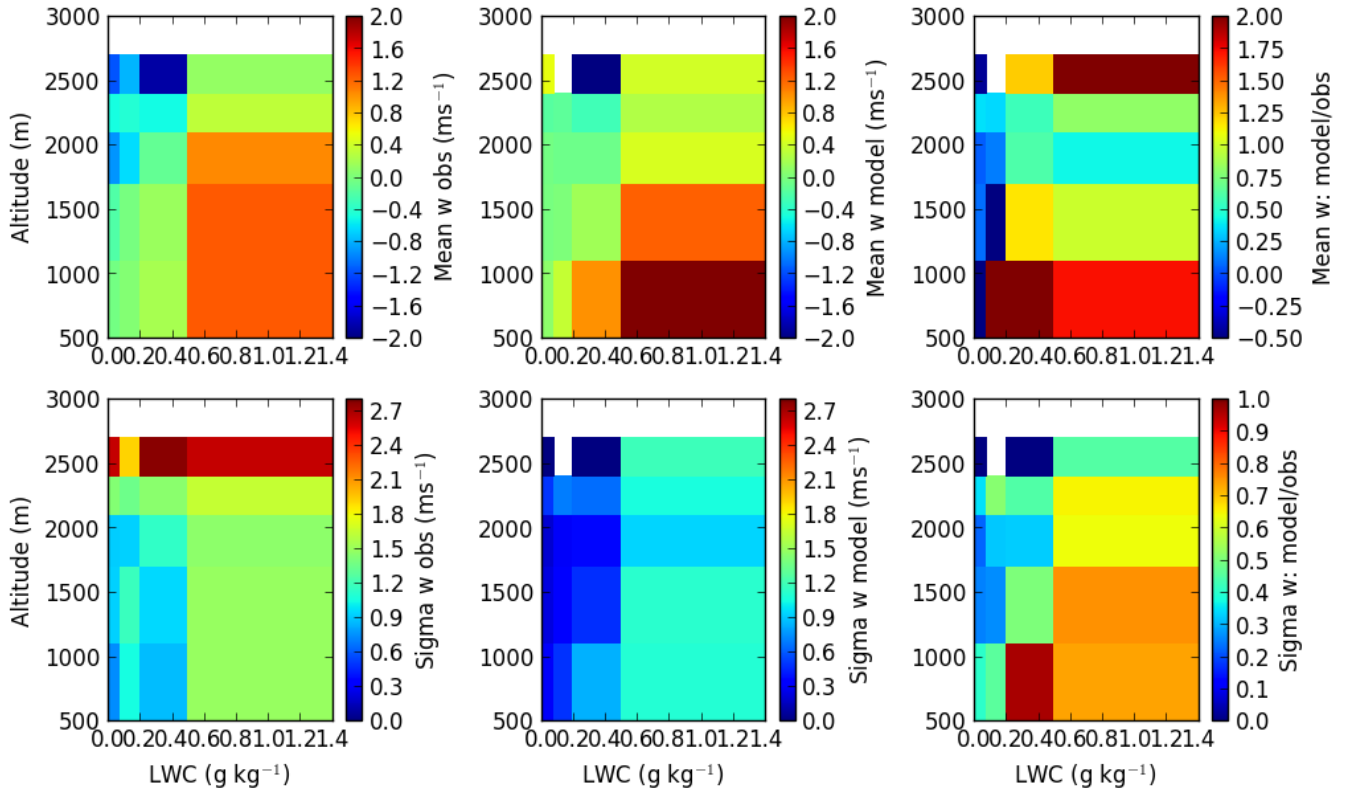


Figure S4. Mean and standard deviation of in-cloud updraft speed in observations and in simulations, at the usual flight altitudes and in bins of liquid water content with boundaries at 0.08, 0.2, and 0.5gkg⁻¹

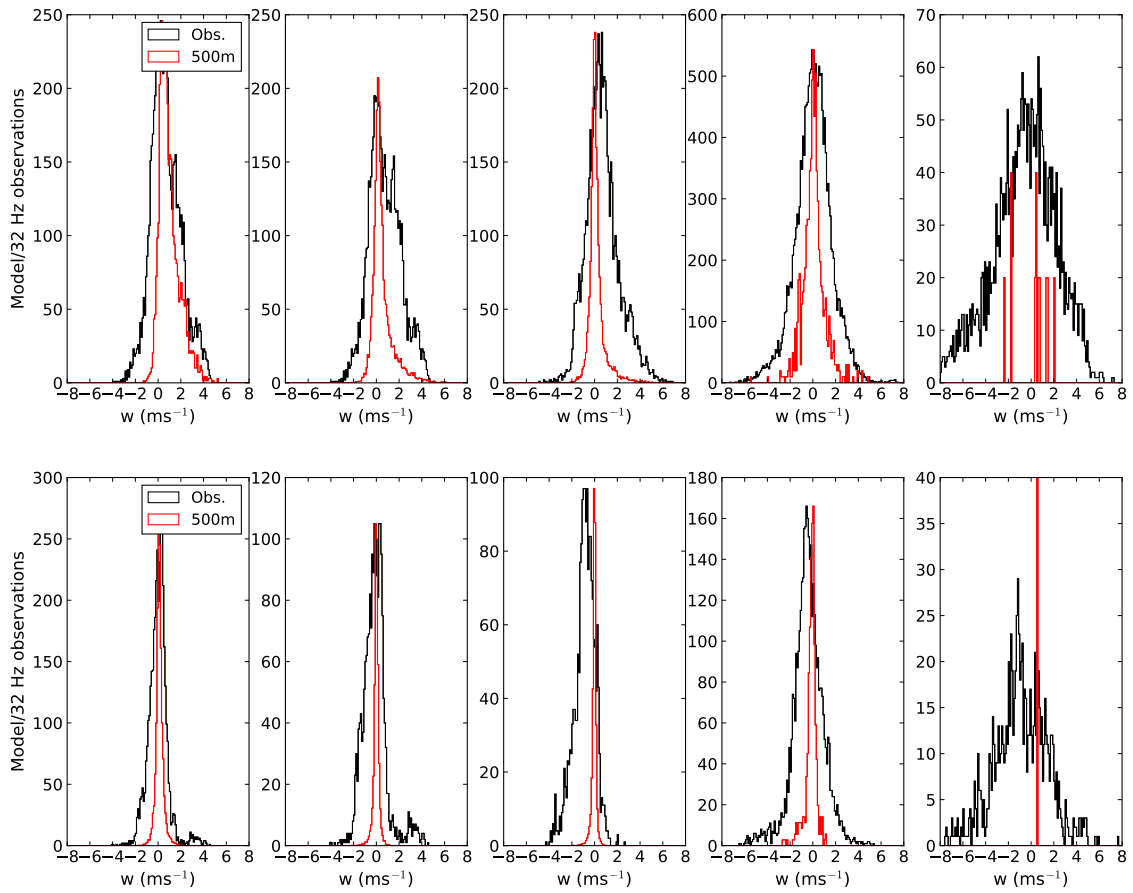


Figure S5. Updraft speeds in model and observations, top for in-cloud $LWC > 0.15 \text{ gkg}^{-1}$ and bottom for $LWC < 0.15 \text{ gkg}^{-1}$

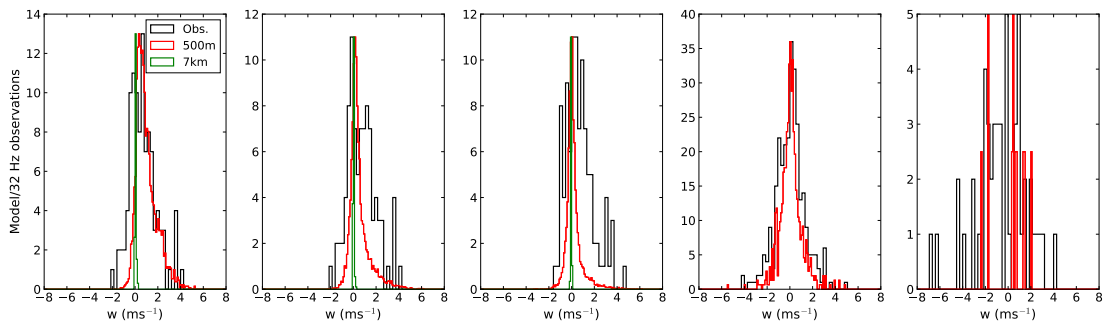


Figure S6. Simulations compared to observed updrafts that have been smoothed out to average over intervals of 500 m, for comparison with the model at this horizontal resolution. Only data for which for in-cloud liquid water content exceeds 0.15 gkg^{-1} are shown.

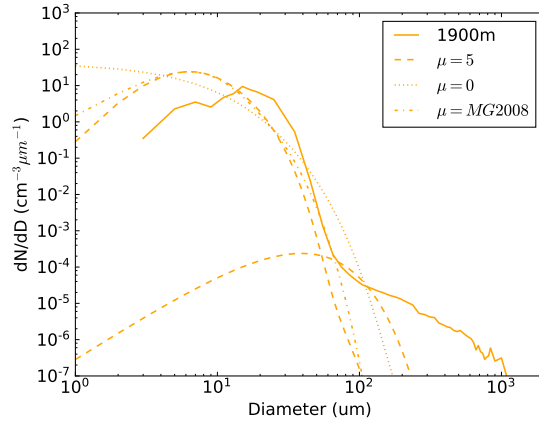


Figure S7. Particle size distributions at 1900 m altitude: observations as in Figure 9, the gamma size distribution with $\mu = 5$ used in this paper (dashed line), the exponential size distribution that was previously in the CASIM code (dotted), and the Morrison and Gettelman (2008) size distribution (dash-dot) that would be derived from the same moments.

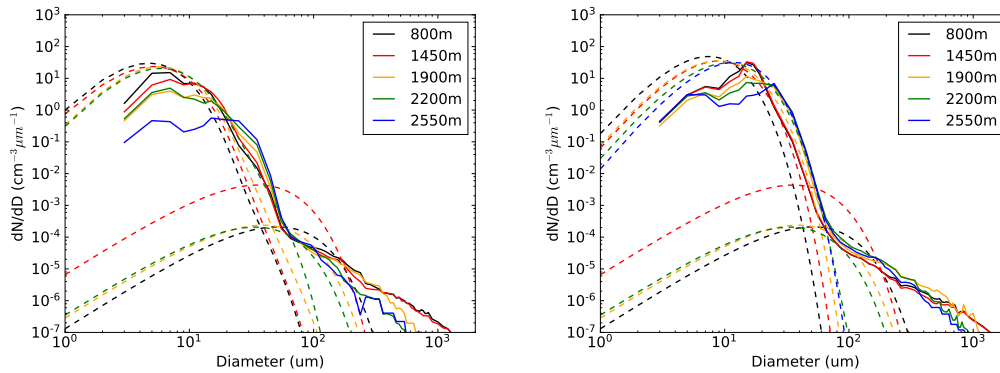


Figure S8. Particle size distributions as Figure 9 except with $LWC < 0.15 \text{ gkg}^{-1}$ (left) and $LWC > 0.15 \text{ gkg}^{-1}$ (right).

Table S3. Change to simulated number mean droplet radius when the exponential size distribution is replaced offline by the size distribution of Morrison and Gettelman (2008), based on the same moments.

Altitude	\bar{r} (exp) (μm)	\bar{r} (MG08) (μm)	\bar{r} ($\mu = 5$) (μm)
800	2.10	3.44	3.29
1450	2.40	3.89	3.76
1900	2.68	4.39	4.21
2215	3.54	5.60	5.56
2550	4.20	6.06	6.59

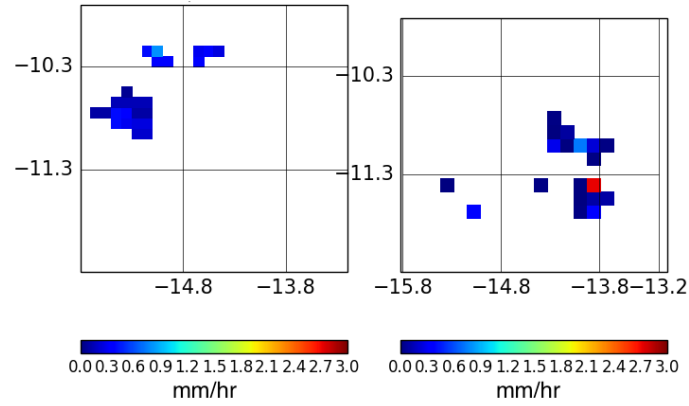


Figure S9. GPM observations of rain (left) compared to simulated rain (right) in the default version of the model.

Table S4. Values of the velocity scaling factor $\sqrt{f/R}$ for a horizontal resolution of 500m, a factor $f = 4$ correction to the vertical velocity variance suggested by Malavelle et al. (2014), and two boundary layer heights representative of the CLARIFY case study.

Boundary layer type	Z_{ml}	$\sqrt{f/R}$ ($Z = 1800\text{m}$)	$\sqrt{f/R}$ ($Z = 2200\text{m}$)
II	$0.5Z$	4.27	3.85
III	$1.3Z$	2.81	2.64
IV	$0.5Z$	4.27	3.85
V (sc)	$0.5Z$	4.27	3.85
V (cbl)	Z	3.09	2.87
VI	Z	3.09	2.87
VII	$0.5Z$	4.27	3.85

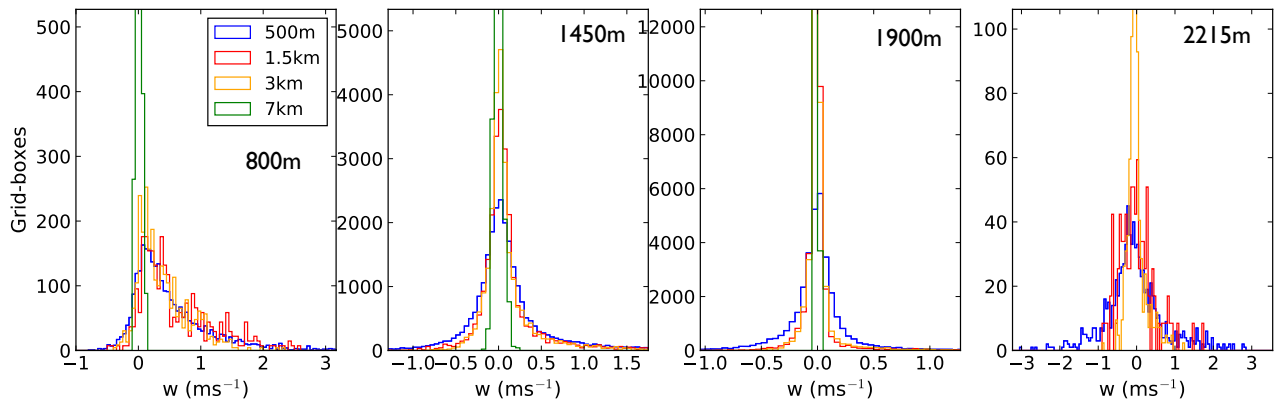


Figure S10. Vertical velocities in simulations at 500 m, 1.5 km and 3 km resolution at the altitudes of the four lower straight and level flight legs, where the sample of in-cloud grid boxes is large enough. No threshold liquid water content is applied, and the x axis range is reduced compared to Figure 6 for clarity.

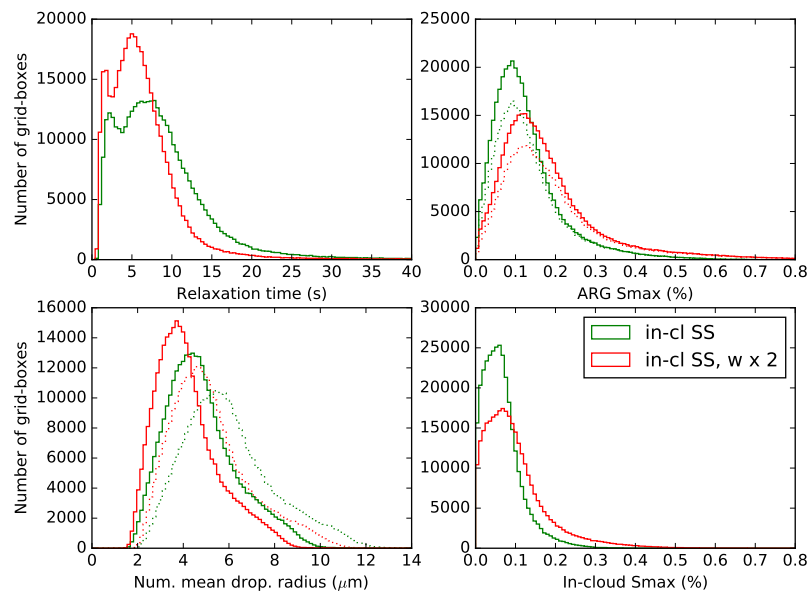


Figure S11. Histograms of grid-box mean relaxation time where relaxation time is used (in grid-boxes where in-cloud quasi-steady supersaturation is used to activate new droplets), ARG maximum supersaturation (on all grid boxes where activation is taking place, and, with dotted lines, on grid boxes where relaxation time is calculated), number mean droplet radius where relaxation time is used, and in-cloud quasi-steady supersaturation where it is used. Dotted lines on the plot of number mean droplet radius show effective radius, which is 25% higher.

The strange UKCA distribution of cloud droplet concentrations

At cloud base, the UKCA cloud droplet number concentration calculation samples a Gaussian PDF with mean equal to the gridbox mean updraft and width equal to the larger of 0.01 and $\sqrt{2/3TKE}$ (Boutle et al., 2018; Mulcahy et al., 2018), where TKE is the unresolved turbulent kinetic energy. A histogram showing the correlation of the droplet number concentration and the vertical velocity for the lowest 900 m in the model (roughly corresponding to cloud base altitudes), is shown in Supplementary Figure S12. The droplet concentrations and updraft speeds are calculated for 20 bins of the PDF and then the weighted mean is taken:

$$N_d = \frac{\sum N_i p(w_i)}{\sum p(w_i)} \quad (S1)$$

Here $p(w_i)$ is the probability a sub-grid updraft takes the value w_i . So far so good, but this procedure is coded such that the minimum updraft ever sampled from the PDF is zero and the maximum number ever sampled is four times the width, *independently of the mean of the PDF*. The maximum value of $\sqrt{2/3TKE}$ is around 1.2 at cloud base but the mean is around 0.15 ms^{-1} , and so, for example, if the mean updraft speed is less than -0.45 ms^{-1} or greater than 1.05 ms^{-1} (both frequent occurrences in the 500 m resolution simulations) and the width is 0.15, the integral of the PDF between 0 and 0.6 will be essentially zero, as this range is always over 3σ from the mean. The cloud droplet concentration that results will be poorly defined, most likely zero, because one is dividing by zero in the denominator (and multiplying by zero in the numerator) of the weighted mean. The droplet concentration is then reset to its hard-coded minimum of 5 cm^{-3} . The characteristic updraft speed, which is the updraft speed sampled from the PDF that would give the same cloud droplet concentration as the actual weighted mean concentration, will be zero if the real updraft speed is large and negative, or around four times the PDF width if the real updraft speed is large and positive.

We conclude that the single-moment UKCA activation scheme should not be used at resolutions where the grid-box mean updraft speed may exceed four times its distribution's width, or that the minimum width should be artificially increased in these situations.

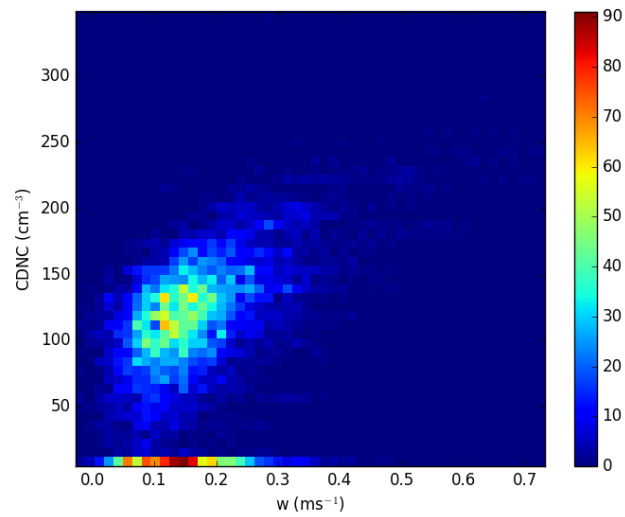


Figure S12. Correlation of updraft with cloud droplet number calculated with the UKCA activation scheme at low altitudes (below 900 m) for the 7 km-resolution simulation. At or close to cloud base, the updrafts can still be significant compared to the minimum updraft width, and consequently the PDF is not always fully sampled. All times are used (not just midday on 19 August) to increase the statistics available.